Optical Review (2018) 25:264–270
https://doi.org/10.1007/s10043-018-0417-4

REGULAR PAPER

Ultraflat and broadband optical frequency comb generator based on cascaded two dual-electrode Mach–Zehnder modulators

Kun Qu[1] · Shanghong Zhao[1] · Xuan Li[1] · Qinggui Tan[2] · Zihang Zhu[1]

Received: 23 September 2017 / Accepted: 17 February 2018 / Published online: 27 February 2018

Abstract
A novel scheme for the generation of ultraflat and broadband optical frequency comb (OFC) is proposed based on cascaded two dual-electrode Mach–Zehnder modulators (DE-MZM). The first DE-MZM can generate a four-comb-line OFC, then the OFC is injected into the second DE-MZM as a carrier, which can increase the number of comb lines. Our modified scheme finally can generate a broadband OFC with high flatness by simply modifying the electrical power and the bias voltage of the DE-MZM. Theoretical analysis and simulation results reveal that a 16-comb-line OFC with a frequency spacing that two times the frequency of the RF signal can be obtained. The power fluctuation of the OFC lines is 0.48 dB and the unwanted-mode suppression ratio (UMSR) can reach 16.5 dB. Additionally, whether the bias drift of the DE-MZMs has little influence on the power fluctuation is also analyzed. These results demonstrate the robustness of our scheme and verify its good accuracy and high stability with perfect flatness.

Keywords Optical frequency comb (OFC) · Dual-electrode Mach–Zehnder modulator · Low power fluctuation · Microwave photonics

1 Introduction

Thanks to the distinct advantages of equal frequency spacing, equal spectral intensity and flexible tunability, the optical frequency comb (OFC) has drawn much attention in various fields, such as frequency domain optical arbitrary wave generation, photonic-assisted analog to digital converters, ultrafast optical signal processing, and dense wavelength division multiplexed transmission systems [1–4]. Therefore, numerous techniques have been demonstrated for OFC generation. There are some OFC generation schemes demonstrated using passive mode-locked erbium-doped fiber laser [5–7]. However, mode-locked sources require complex and rigorous phase locking arrangements to maintain stability. The OFC generators based on fiber nonlinearities have also been proposed in [8], but this technique needs high optical amplifiers and complicated structures. Methods for OFC generation based on modulation of a continuous wave (CW) laser using electro-optic modulator have been widely investigated due to the advantages of simplicity and stability [9–12]. For this method, a single modulator can be used to generate OFC [13], and the system is simple, but the number of comb lines is limited. The number of the comb lines can be increased by cascaded modulators. For example, cascaded intensity and phase modulators can be used to generate an OFC with 42 comb lines, but the power of the driven signal is too high for practical application [10].

To overcome the problems mentioned above, some methods have been proposed [14–16]. A two-stage OFC generator based on polarization modulators and a Mach–Zehnder interferometer is proposed in [14], it can generate flat OFCs with a large number of comb lines. However, the power fluctuation is more than 1 dB. Method that cascaded two chirping of Mach–Zehnder modulators to generate OFCs is proposed [15]. This scheme generated OFCs by changing chirp factor and the best quality of OFC has 27 comb lines with the power fluctuation that less than 1 dB, but when the chirp factor is changed, the power fluctuation will be more than 2 dB. Ref. [16] proposed a scheme that cascaded two polarization modulators and a polarizer to generate an ultraflat OFC with the comb flatness within 1 dB; however, the UMSR at most is 10.8 dB and the state of polarization

✉ Kun Qu
m13259463680@163.com

[1] Air Force Engineering University, Xi'an, China

[2] China Academy of Space Technology, Xi'an 710000, China

is difficult to control. Additionally, for the traditional OFC generator and the schemes that are mentioned above, the frequency spacing of the OFC lines is equal to the frequency of the RF signal, so the bandwidth of the OFC is insufficient.

In this paper, we propose an ultraflat and broadband OFC generator based on cascaded two DE-MZMs. This scheme can be investigated using a two-stage structure, where the first stage is configured to generate an OFC with four comb lines by a DE-MZM, then this OFC is injected into the second stage as a carrier, and in the second stage we also use a DE-MZM as the same form as the first stage, which could further increase the comb lines. Compared with the previous reports, our scheme can meet the requirement of large bandwidth thanks to the 16 comb lines with a frequency spacing two times the frequency of the RF signal. At the same time, the power fluctuation of the OFC is less than 0.5 dB, which is immune from the bias drift of the DE-MZMs. By developing a mathematical model and performing simulations on OptiSystem software, the power fluctuation of the generated OFC is 0.48 dB and the UMSR is 16.5 dB. When the frequency of RF signal changed, we can also get an OFC with the power fluctuation and the UMSR of 0.48 and 16.2 dB, respectively. Additionally, it is manifest that the bias drift of the MZMs has little influence on the property of OFC. It is shown that the generated OFC is broadband, ultraflat and highly stable.

2 Operating principle

In this section, we present a mechanistic modeling diagram and introduce the operating principle of the proposed scheme. The schematic diagram of the proposed OFC generator is shown in Fig. 1, which consists of a CW laser, two DE-MZMs (MZM1 and MZM2) and two RF signals (RF1 and RF2). Figure 2 shows the configuration of DE-MZM, which has a dual electrode (separate DC and RF), v_{rf1} and

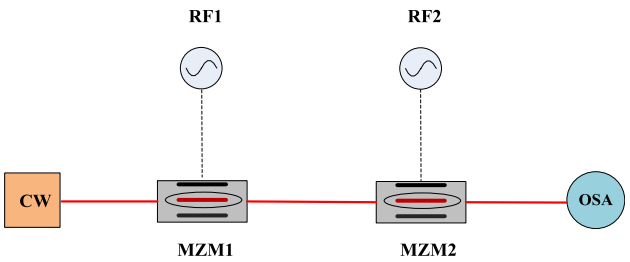

Fig. 1 Schematic diagram of our proposed OFC generator

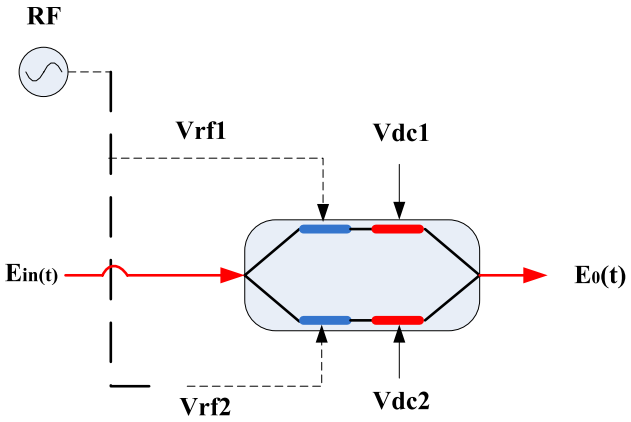

Fig. 2 Configuration of the dual-electrode MZM

v_{rf2} are the RF voltages to the upper and lower arms of the MZM, respectively. v_{dc1} and v_{dc2} are the DC voltages to the upper and lower arms of the MZM, respectively.

Assume that the optical signal applied to the input port of MZM1 is

$$E_{in}(t) = E_0 e^{j\omega_0 t} \tag{1}$$

where E_0 and ω_0 are the amplitude and the angular frequency of the input optical signal, respectively. The corresponding output optical field from MZM1 can be expressed as

$$E_{out}(t) = \frac{1}{2}E_{in}(t)\left\{ e^{j\left[\pi \frac{V_{1(t)}}{V_\pi}\right]} + e^{j\left[\pi \frac{V_{2(t)}}{V_\pi}\right]} \right\} \tag{2}$$

where v_π is the half-wave voltage of the MZM. $V_1(t)$ and $V_2(t)$ are the electrical driving signals supplied to the upper and lower arms of MZM1, respectively, and we assume that

$$V_1(t) = V_{dc1} + V_{rf1}\cos(\omega_{rf1}t + \varphi_1) \tag{3}$$

$$V_2(t) = V_{dc2} + V_{rf2}\cos(\omega_{rf2}t + \varphi_2) \tag{4}$$

where φ_1 and φ_2 are the static phase of the two electrical driving signals, ω_{rf1} and ω_{rf2} are the angular frequency of the two driving signals. Then Eq. (2) can be expressed as

$$E_{out}(t) = \frac{1}{2}E_0 e^{j\omega_0 t}\left\{ e^{j\left[\pi \frac{V_{dc1}+V_{rf1}\cos(\omega_{rf1}t+\varphi_1)}{V_\pi}\right]} + e^{j\left[\pi \frac{V_{dc2}+V_{rf2}\cos(\omega_{rf2}t+\varphi_2)}{V_\pi}\right]} \right\} \tag{5}$$

Finally, when $V_{rf1} = V_{rf2}$, $\omega_{rf1} = \omega_{rf2}$. Equation (5) can be expressed using Bessel functions as

$$
\begin{aligned}
E_{\text{out}}(t) &= \frac{1}{2}E_0 e^{j\omega_0 t} e^{j\left[\pi \frac{V_{\text{dc1}}+V_{\text{dc2}}}{2V_\pi}\right]} \sum_{n=-\infty}^{+\infty} J_n(m) e^{jn\left[\omega_{rf}t+\frac{\varphi_1+\varphi_2+\pi}{2}\right]} \cos\left[\pi\frac{V_{\text{dc1}}-V_{\text{dc2}}}{2V_\pi} + n\frac{\varphi_1-\varphi_2}{2}\right] \\
&= \frac{1}{2}E_0 e^{j\omega_0 t} e^{j\left[\pi \frac{V_{\text{dc1}}+V_{\text{dc2}}}{2V_\pi}\right]} \left\{ J_0(m)\cos\left[\pi\frac{V_{\text{dc1}}-V_{\text{dc2}}}{2V_\pi}\right] \right. \\
&\quad + J_1(m) e^{j\left[\omega_{rf}t+\frac{\varphi_1+\varphi_2+\pi}{2}\right]} \cos\left[\pi\frac{V_{\text{dc1}}-V_{\text{dc2}}}{2V_\pi} + \frac{\varphi_1-\varphi_2}{2}\right] \\
&\quad + J_{-1}(m) e^{-j\left[\omega_{\text{rf}}t+\frac{\varphi_1+\varphi_2+\pi}{2}\right]} \cos\left[\pi\frac{V_{\text{dc1}}-V_{\text{dc2}}}{2V_\pi} - \frac{\varphi_1-\varphi_2}{2}\right] \\
&\quad + J_2(m) e^{j2\left[\omega_{\text{rf}}t+\frac{\varphi_1+\varphi_2+\pi}{2}\right]} \cos\left[\pi\frac{V_{\text{dc1}}-V_{\text{dc2}}}{2V_\pi} + \varphi_1-\varphi_2\right] \\
&\quad \left. + J_{-2}(m) e^{-2j\left[\omega_{\text{rf}}t+\frac{\varphi_1+\varphi_2+\pi}{2}\right]} \cos\left[\pi\frac{V_{\text{dc1}}-V_{\text{dc2}}}{2V_\pi} - (\varphi_1-\varphi_2)\right] + \ldots \right\}
\end{aligned} \tag{6}
$$

Equation (6) shows that the Bessel functions affect the sidebands of the optical field, in which $m = \frac{\pi V_{\text{rf}}}{V_\pi}$. When $V_{\text{dc1}} - V_{\text{dc2}} = \pm V_\pi$, the MZM biased at minimum transmission point, the optical carrier can be well suppressed, and when $V_{\text{dc1}} - V_{\text{dc2}} = \pm V_\pi$ and $\varphi_1 - \varphi_2 = \pm\pi$, the even-order sidebands can be well suppressed. However, this is the ideal case, the optical carrier and the even-order sidebands cannot be completely suppressed due to the influence of the extinction ratio of the MZM. Then Eq. (6) can be expressed as

Then, the generated OFC1 is injected into MZM2 as a carrier, where a 16-comb-line OFC finally can be generated. This process can be described as in Fig. 3, when the OFC1 with 4 lines is injected into MZM2, which is driven by RF2 with a frequency that is a quarter of the RF1. Based on the same principle as described in Eq. (5)–(7), per line of OFC1 can generate four lines in MZM2. As a result, 16 flat comb lines can be achieved based on cascaded two MZMs, which frequency spacing is twice of the frequency of RF2.

$$
\begin{aligned}
E_{\text{out}}(t) &= \frac{1}{2}E_0 e^{j\omega_0 t} e^{j\left[\pi \frac{V_{\text{dc1}}+V_{\text{dc2}}}{2V_\pi}\right]} \left\{ J_{\pm1}(m) e^{\pm j\left[\omega_{\text{rf}}t+\frac{\varphi_1+\varphi_2+\pi}{2}\right]} \cos\left[\pi\frac{V_{\text{dc1}}-V_{\text{dc2}}}{2V_\pi} \pm \frac{\varphi_1-\varphi_2}{2}\right] \right. \\
&\quad + J_{\pm3}(m) e^{\pm 3j\left[\omega_{\text{rf}}t+\frac{\varphi_1+\varphi_2+\pi}{2}\right]} \cos\left[\pi\frac{V_{\text{dc1}}-V_{\text{dc2}}}{2V_\pi} \pm \frac{3(\varphi_1-\varphi_2)}{2}\right] \\
&\quad + \frac{1}{\sqrt{10^{\frac{r}{10}}}}\left[J_0(m)\cos\left(\pi\frac{V_{\text{dc1}}-V_{\text{dc2}}}{2V_\pi}\right) \right. \\
&\quad + J_{\pm1}(m) e^{\pm j\left[\omega_{\text{rf}}t+\frac{\varphi_1+\varphi_2+\pi}{2}\right]} \cos\left[\pi\frac{V_{\text{dc1}}-V_{\text{dc2}}}{2V_\pi} \pm \frac{\varphi_1-\varphi_2}{2}\right] \\
&\quad + J_{\pm2}(m) e^{\pm 2j\left[\omega_{\text{rf}}t+\frac{\varphi_1+\varphi_2+\pi}{2}\right]} \cos\left[\pi\frac{V_{\text{dc1}}-V_{\text{dc2}}}{2V_\pi} \pm \varphi_1-\varphi_2\right] + \cdots \\
&\quad \left. \left. + J_{\pm n}(m) e^{\pm nj\left[\omega_{\text{rf}}t+\frac{\varphi_1+\varphi_2+\pi}{2}\right]} \cos\left[\pi\frac{V_{\text{dc1}}-V_{\text{dc2}}}{2V_\pi} \pm \frac{n(\varphi_1-\varphi_2)}{2}\right] \right] \right\}
\end{aligned} \tag{7}
$$

where r is the extinction ratio of the MZM, it can be seen that when the extinction ratio is much bigger than 10, the Bessel functions of $J_0(m)$ and $J_2(m)$ can be ignored, but in fact, the extinction ratio is always between 20 and 30 dB, the optical carrier and the second-order sidebands cannot be completely suppressed. When $m = 3.03$, $J_1(m) = 0.327$ and $J_3(m) = 0.3178$, $J_1(m) \approx J_3(m)$. $J_5(m) = 0.0049$, thus the items of Bessel function that are higher than $J_5(m)$ can be ignored. Finally, an OFC with four comb lines whose frequency spacing is two times the frequency of RF1 can be generated in MZM1, here we called it OFC1.

3 Results and discussion

To investigate the performance of the proposed OFC generator, a simulation is conducted using Optisystem, and the results are then compared with the mathematical analysis. In our setup, the CW laser is operated at 1552.52 nm with a power of 10 dBm and a linewidth of 100 kHz, the half-wave voltage for the MZMs is 3V. RF1 operated at 16 GHz with 24.08 dBm, while RF2 operated at 4 GHz with 12.04 dBm. To fit the facts, the extinction ratio of the MZM is set as 20 dB.

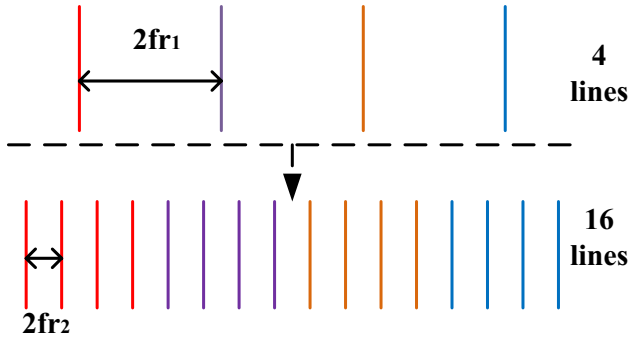

Fig. 3 Schematic diagram of 16 comb-line generation

The results of the generated OFC in the optical spectra analyzer are depicted as follows: when only RF1 is enabled, the optical spectra at the output of MZM1 are shown in Fig. 4. It can be seen that an OFC with four comb lines is generated and the frequency spacing is 32 GHz, which is two times the frequency of RF1; the power fluctuation and the UMSR are 0.25 and 16.5 dB, respectively.

Then this OFC is sent to MZM2 as a carrier. Finally, the optical spectra at the output of the scheme are shown in Fig. 5; it can be clearly seen that an OFC with 16 comb lines is generated. The frequency spacing of the OFC is two times the frequency of RF2, which is 8 GHz, and the power fluctuation and UMSR are 0.48 and 16.5dB, respectively. These results are consistent with the mathematical analysis that is obtained in Sect. 2, and the generated OFC shows good performance.

Additionally, our modified scheme inherits the merit of tunable frequency spacing. Because the scheme has no wavelength filtering in the optical domain or frequency filtering in the electrical domain, the frequency spacing of the OFC is widely tunable. Figure 6 shows the optical spectra of the generated OFC with a frequency spacing of 7 GHz, the power fluctuation and UMSR are 16.2 and 0.48 dB, respectively. Thus, it can be seen that the generated OFC is very stable with good frequency spacing tunability. The power loss is mainly introduced from a modulation loss

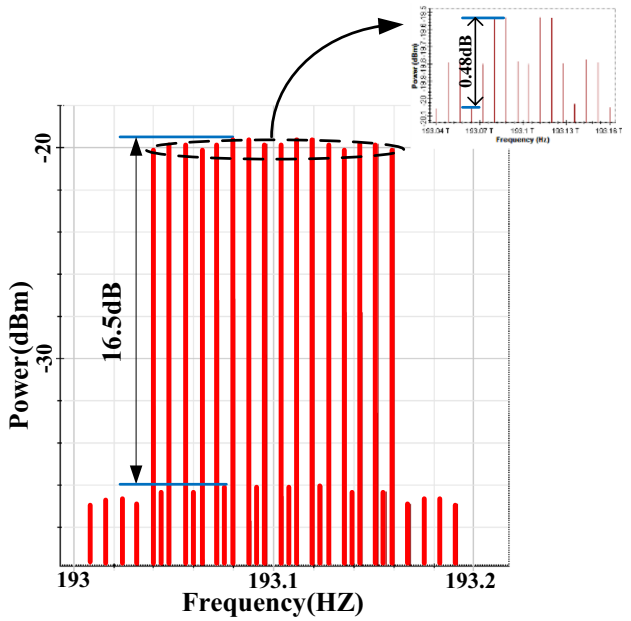

Fig. 5 Optical spectra of 16-line OFC with a spacing of 8 GHz

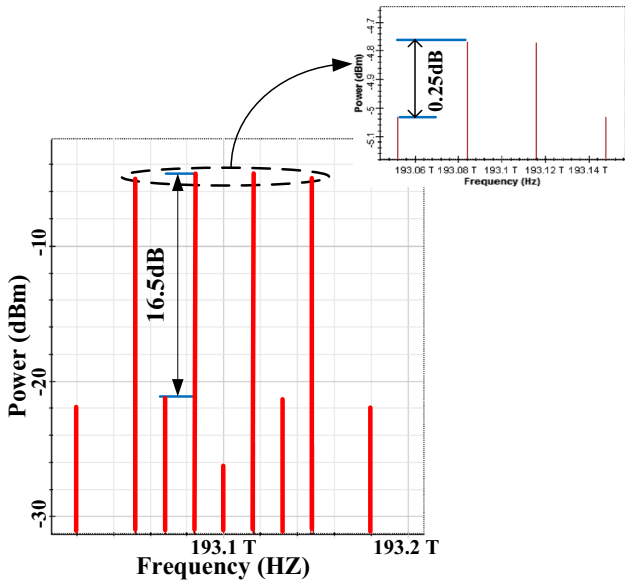

Fig. 4 Optical spectra of 4-line OFC with a spacing of 32 GHz

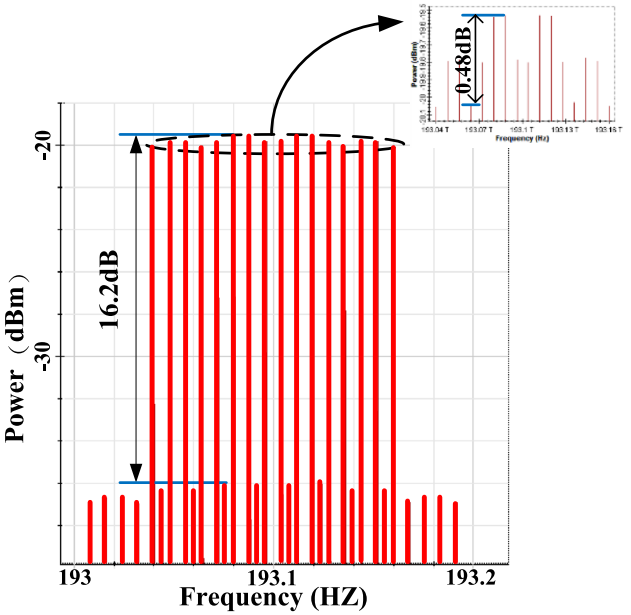

Fig. 6 Optical spectra of 16-line OFC with a spacing of 7 GHz

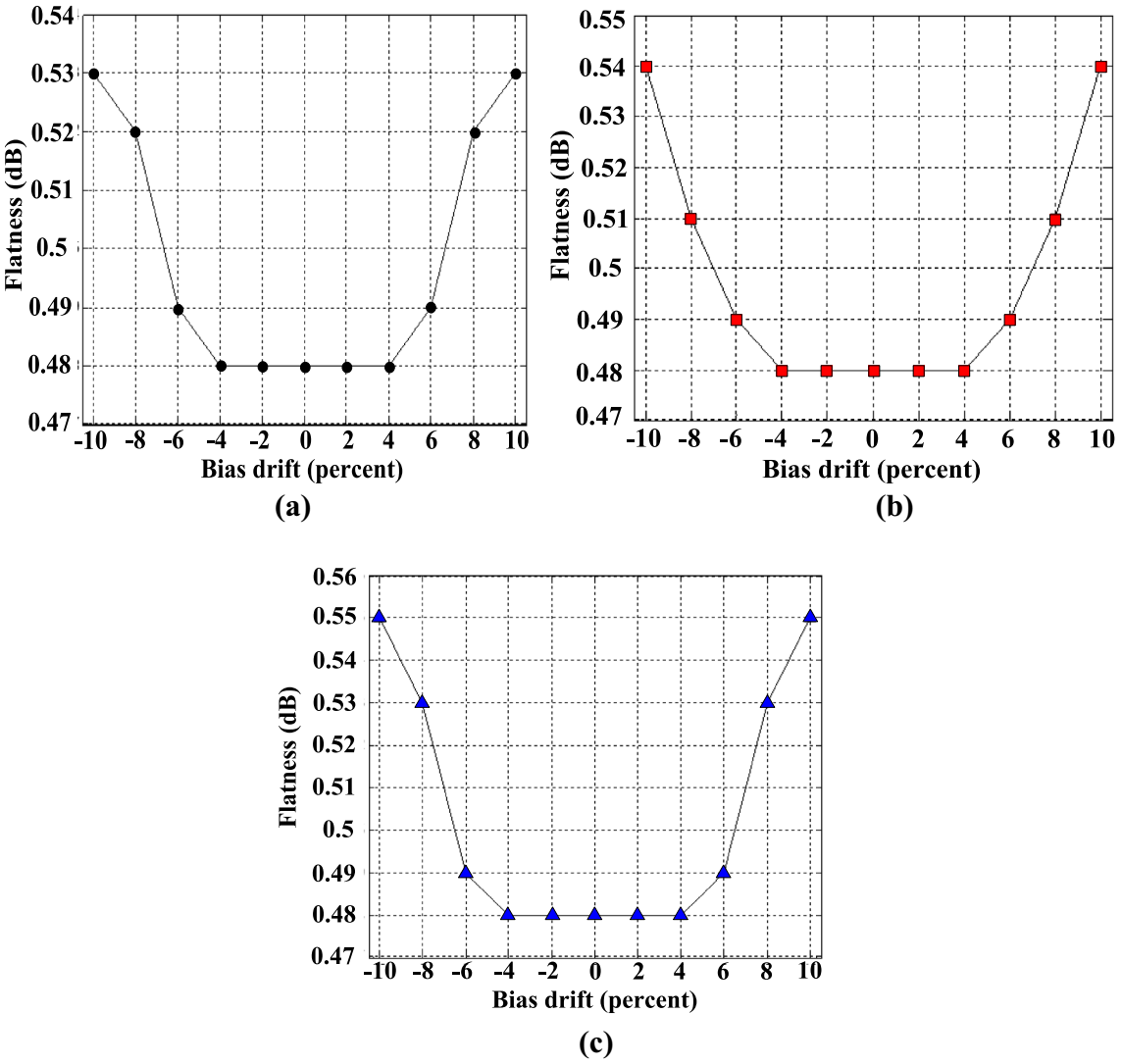

Fig. 7 **a** The influence of bias drift from MZM1 on flatness. **b** The influence of bias drift from MZM2 on flatness. **c** The influence of bias drift from both MZM1 and MZM2 on flatness

$\alpha_1 = 10 \times \frac{\log\left\{\left(\frac{J_1(m)\cos(\pi V_b)}{2}\right)^2\right\}}{\log(10)} = -8$ dB and an insertion loss $\alpha_2 = 5 \sim 7$ dB of the MZMs, and it can be compensated by an erbium-doped fiber amplifier (EDFA) at the output of the MZM2.

According to the analysis in Sect. 2, one of the conditions that should be satisfied to generate the OFC is $V_{dc1} - V_{dc2} = \pm V_\pi$. However, there is a problem that the MZM has bias voltage drift when it works, so it is necessary to analyze the influence on the performance of the OFC caused by bias drift. Figure 7a shows the influence of bias drift from MZM1 on the flatness of the generated OFC, it can be seen the flatness of the OFC almost has no change when the bias drift is between -4 and 4%, even when the bias drift is at ± 10%, the flatness of the OFC is no more than 0.53 dB. Figure 7b shows the influence of bias drift from MZM2 on the flatness of the generated OFC, we can see that the flatness of the OFC also has no change when the bias drift is between -4 and 4%, and when the bias drift is at ± 10%, the flatness of the OFC is no more than 0.54 dB. Figure 7c shows the change of flatness when both MZM1 and MZM2 have bias drift, it can be seen when both MZM1 and MZM2 have bias drift between -4 and 4%, the flatness of the OFC also has no change, which is 0.48 dB, when the two MZMs have bias drift at ± 10%, the flatness of the OFC is no more than 0.55 dB.

Figure 8a shows the influence of bias drift from MZM1 on the UMSR of the generated OFC, it can be seen the UMSR of the OFC almost has no change when the bias

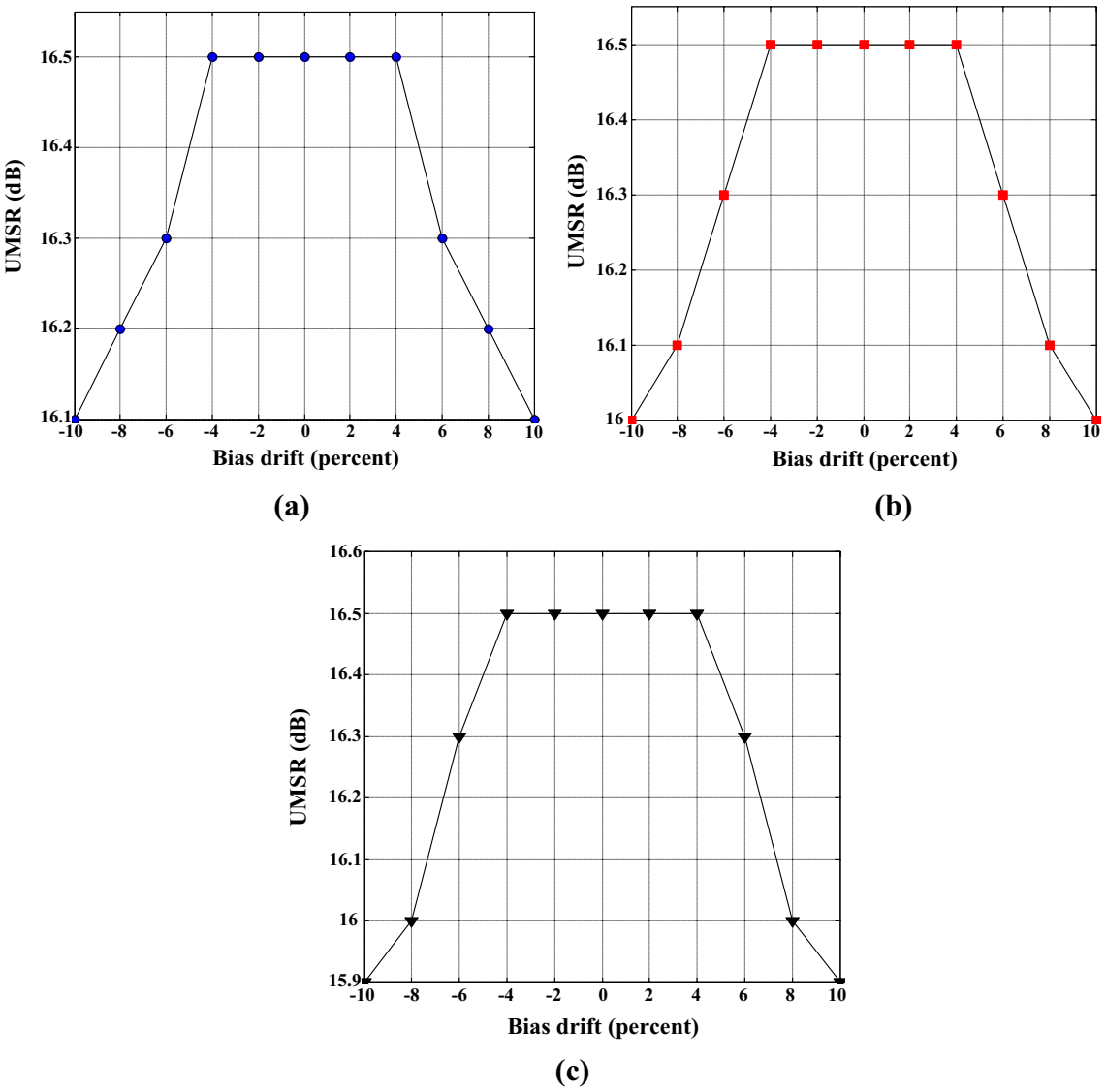

Fig. 8 **a** The influence of bias drift from MZM1 on UMSR. **b** The influence of bias drift from MZM2 on UMSR. **c** The influence of bias drift from both MZM1 and MZM2 on UMSR

drift is between −4 and 4%, even when the bias drift is at ±10%, the UMSR of the OFC is no less than 16.1 dB. Figure 8b shows the influence of bias drift from MZM2 on the UMSR of the generated OFC, we can see that the UMSR of the OFC also has no change when the bias drift is between −4 and 4%, and when the bias drift is at ±10%, the UMSR of the OFC is no less than 16 dB. Figure 8c shows the change of UMSR when both MZM1 and MZM2 have bias drift, it can be seen when both MZM1 and MZM2 have bias drift between −4 and 4%, the UMSR of the OFC also has no change, which is 16.5 dB, when the two MZMs have bias drift at ±10%, the UMSR of the OFC is no less than 15.9 dB. Therefore, these results show that the generated OFC has a good performance.

4 Conclusion

In this work, we have presented a novel scheme to generate an ultraflat and broadband optical frequency comb, which is based on cascaded two dual-electrode Mach–Zehnder modulators. The two MZMs are configured as the same form, while the first MZM is driven by RF1 and the second MZM is driven by RF2. RF1 and RF2 have the same power but the frequency of RF2 is quarter of RF1. By simply adjusting the electrical powers and the same bias voltages of MZM1 and MZM2, an OFC with 16 comb lines can be generated. The most distinctive feature of our scheme is the capability to generate a large bandwidth OFC, whose frequency spacing is two times the frequency of the RF signal. Additionally, the generated OFC is highly stable, with 0.48 dB low

power fluctuation and 16.5 dB unwanted-mode suppression ratio. When the frequency of RF1 and RF2 is changed, the frequency spacing is tunable and has no influence on the flatness and the unwanted-mode suppression ratio, which verified the robustness of the proposed structure. The results demonstrate a tunable and stable approach for OFC generation.

Acknowledgements This research was supported by the National Natural Science Foundation of China (Nos. 61231012 and 61401502).

References

1. Cundiff, S.T., Weiner, A.M.: Optical arbitrary waveform generation. Nat. Photonics **4**(11), 760–766 (2010)
2. Sherman, A., Horowitz, M., Zach, S.: Optical under-sampling by using abroadband optical comb with a high average power. Opt. Express **13**, 15502–15513 (2014)
3. Schnatz, H., Lipphardt, B., Degenhardt, C., Peik, E., Schneider, T., Sterr, U., et al.: Optical frequency measurements using fs-comb generators. IEEE Trans. Instrum. Meas. **54**(2), 750–753 (2005)
4. Chen, C., Zhang, C., Zhang, W., Jin, W., Qiu, K.: Scalable and reconfigurable generation of flat optical comb for WDM-based next-generation broadband optical access networks. Opt. Commun. **321**, 16–22 (2014)
5. Stefan, P., Norman, W., Thomas, S.: Flat, rectangular frequency comb generation with tunable bandwidth and frequency spacing. Opt. Lett. **39**(6), 1637–1640 (2014)
6. Diddams, S.A.: The evolving optical frequency comb. J. Opt. Soc. Am. B **27**(11), B51-B62 (2010)
7. Wiberg, A.O.J., Liu, L., Tong, Z.: Photonic preprocessor for analog-to-digital-converter using a cavity-less pulse source. Opt. Express. **20**, 419–427 (2012)
8. Tang, J., Sun, J., Zhao, L., Chen, T., Huang, T., Zhou, Y.: Tunable multiwavelength generation based on Brillouin–erbium comb fiber laser assisted by multiple four-wave mixing processes. Opt. Express **19**(5), 14682–14689 (2011)
9. Zhang, F., Wu, J., Li, Y., Lin, J.: Flat optical freqeuncy comb generation and its application for optical waveform generation. Opt. Commun. **290**(1), 37–42 (2013)
10. Shang, L., Wen, A., Lin, G.: Optical frequency comb generation using two cascaded intensity modulators. J. Opt. **16**(3), 035401 (2014)
11. Shang, L., Wen, A., Lin, G., Gao, Y.: A flat and broadband optical frequency comb with tunable bandwidth and frequency spacing. Opt. Commun. **331**, 262–266 (2014)
12. Metcalf, A.J., Torres-Company, V., Leaird, D.E., Weiner, A.M.: High-power broadly tunable electrooptic frequency comb generator. IEEE J. Sel. Top. Quantum Electron. **19**(6), 3500306–3500311 (2013)
13. Wang, Q., Huo, L., Xing, Y., Zhou, B.: Ultra-flat optical frequency comb generator using a single-driven dual-parallel Mach–Zehnder modulator. Opt. Lett. **39**(10), 3050–3053 (2014)
14. Zhang, F., Ge, X., Pan, S.: A two-stage optical frequency comb generator based on polarizationmodulators and a Mach–Zehnder interferometer. Opt. Commun. **354**, 94–102 (2015)
15. Hmood, J.K., Emami, S.D., Noordin, K.A.: Optical frequency comb generation based on chirping of Mach–Zehnder modulators. Opt. Commun. **344**, 139–146 (2015)
16. He, C., Pan, S.: Ultraflat optical frequency comb generated based on cascaded polarization modulators. Opt. Lett. **37**, 3834–3846 (2012)